

## FLARE GENESIS EXPERIMENT: MAGNETIC TOPOLOGY OF ELLERMAN BOMBS

Schmieder B.<sup>1</sup>, Pariat E.<sup>1</sup>, Aulanier G.<sup>1</sup>, Georgoulis M.K.<sup>2</sup>, Rust D.M.<sup>2</sup>, and Bernasconi P.N.<sup>2</sup>

<sup>1</sup>Observatoire de Paris, LESIA, 92195 Meudon Cedex Principal, France

<sup>2</sup>JHU/Applied Physics Laboratory, 11100 John Hopkins Road, Laurel MD 20723-6099, USA

### ABSTRACT

Flare Genesis Experiment (FGE), a balloon borne Observatory was launched in Antarctica on January 10 2000 and flew during 17 days. FGE consists of an 80 cm Cassegrain telescope with an F/1.5 ultra-low-expansion glass primary mirror and a crystalline silicon secondary mirror. A helium-filled balloon carried the FGE to an altitude of 37 km (Bernasconi et al. 2000, 2001). We select among all the observations a set of high spatial and temporal resolution observations of an emerging active region with numerous Ellerman bombs (EBs). Statistical and morphology analysis have been performed. We demonstrate that Ellerman bombs are the result of magnetic reconnection in the low chromosphere by a magnetic topology analysis. The loci of EBs coincide with “bald patches” (BPs). BPs are regions where the vector field is tangential to the boundary (photosphere) along an inversion line. We conclude that emerging flux through the photosphere is achieved through resistive emergence of U loops connecting small  $\Omega$  loops before rising in the chromosphere and forming Arch Filament System (AFS).

Key words: Solar magnetic field, Ellerman Bombs, flux emergence.

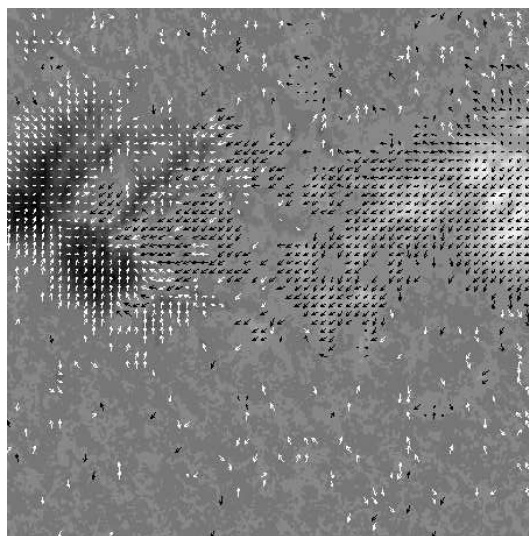


Figure 1. Vector magnetic field from FGE at 17:52:24 UT. White/black arrows representing  $B_{tran}$  are drawn over negative/positive polarities ( $B_{long}$ ).

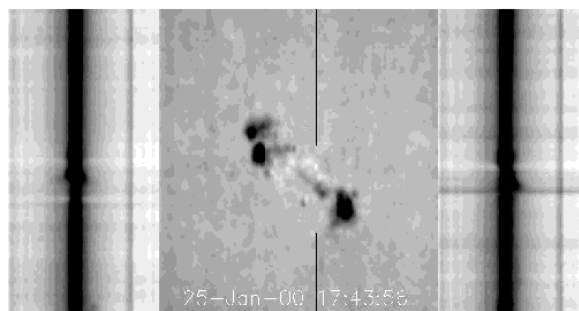


Figure 2. Spectra of Ellerman bombs of AR 8844 (Courtesy of Labonte)

### 1. VECTOR MAGNETOGRAMS AND $H\alpha$ IMAGES

The observations were obtained through a polarization analyser unit (two liquid-crystal variable retarders and a linear polarizing filter, a selection

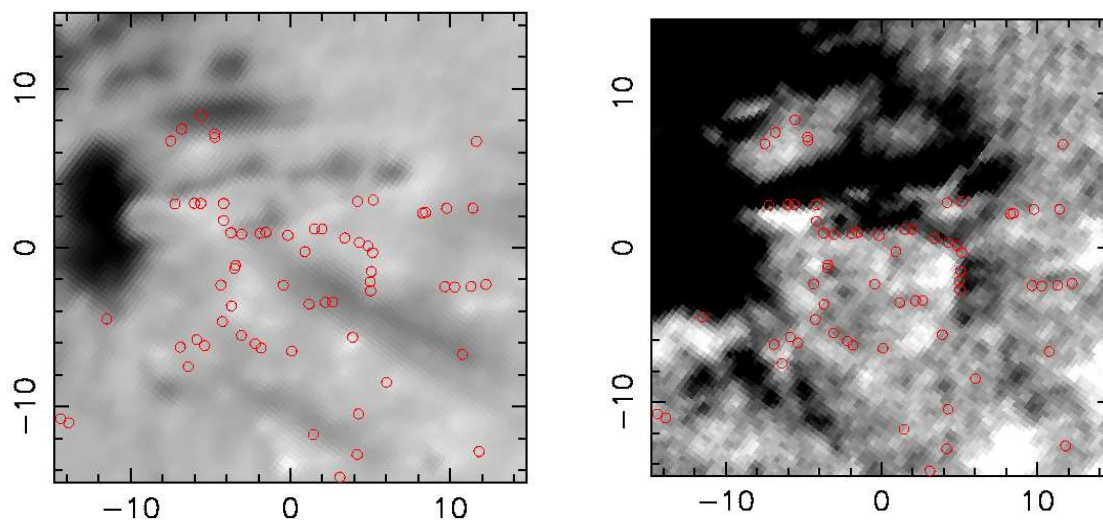


Figure 3. Zoom of observed “Bald Patches” in the trailing spot and the forward supergranules overlaid the  $H\alpha$  map (left panel) and  $B_{long}$  map (threshold of  $B_{trans} = 250$  G) (right panel). The Bald patches are represented by black circles. They fit well some Ellerman Bombs: bright features in the  $H\alpha$  map. Some correspond to the moving features towards the trailing spot in the middle of the supergranule described in Bernasconi et al. (2002).

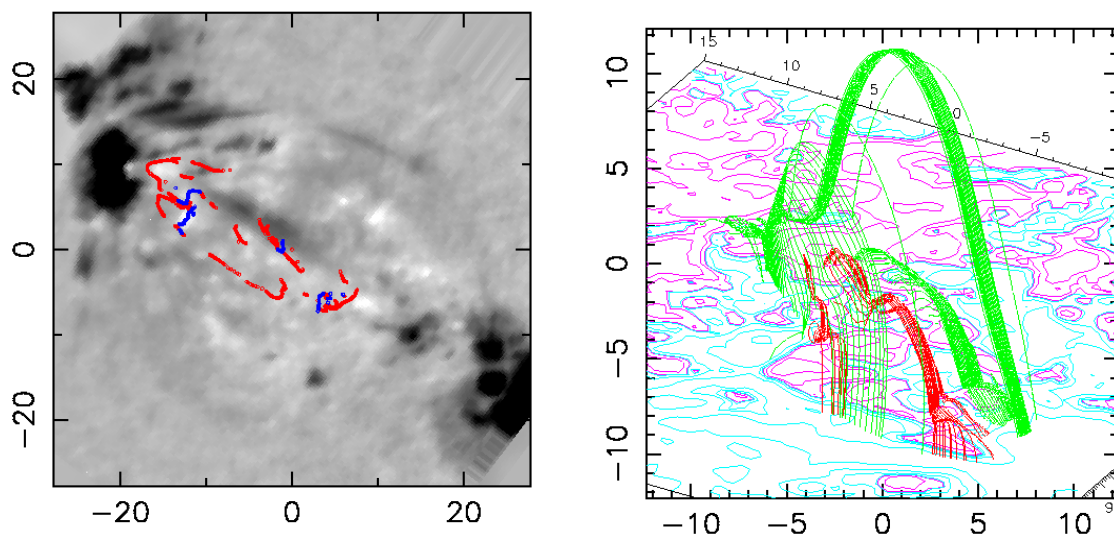


Figure 4. Example of “Bald Patches” (dark lines) and separatrices (grey lines) overlaid on the  $H\alpha$  map (left panel) at 18:00 UT. The bald patches and the separatrices fit well with the Ellerman Bombs: bright features in the  $H\alpha$  map. Example of magnetic field lines joining bald patches and separatrices overlaid  $B_z$  magnetic field (right panel). North is up

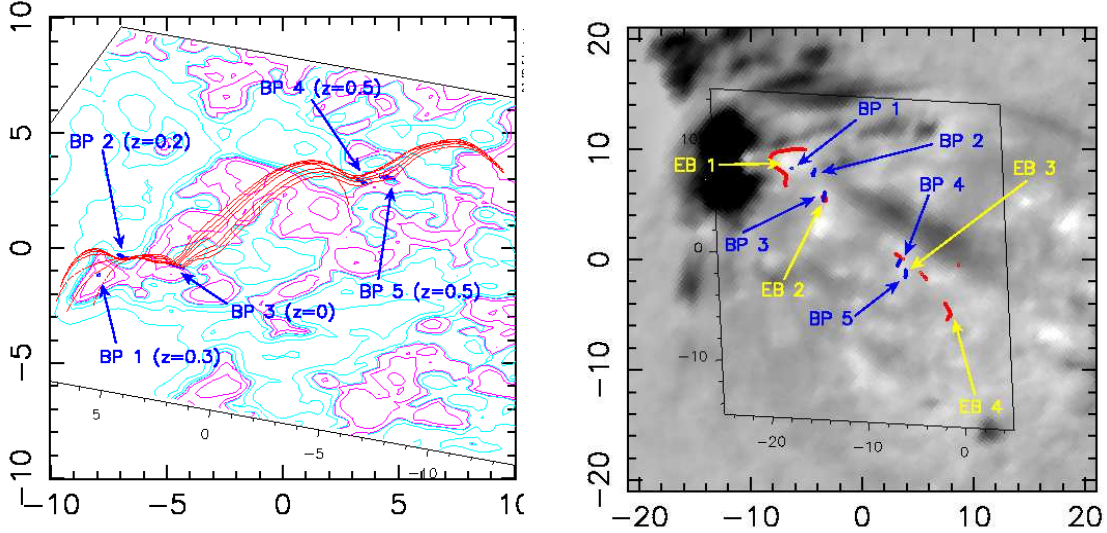


Figure 5. Exemple of “sea serpent” joining Bald Patches” (dark lines) and separatrices (grey lines) overlaid on FGE magnetogram (left panel) at 18:00 UT. The bald patches and the separatrices are overlaid on  $H\alpha$  image (right panel)

of  $1.25 \text{ \AA}$  order-isolation filters, a  $0.16 \text{ \AA}$  tunable Fabry-Pérot etalon filter and refractive optics to present a  $160''$  diameter section of the sun to a  $1024 \times 1024$ -pixel CCD camera. The plate scale is  $0.091''$  per pixel and the image quality was around  $0.5''$ . We made observations of all the four Stokes parameters in the red and blue wings of the Ca I line at  $6122.2 \text{ \AA}$ . Unpolarized observations were obtained at  $0.8 \text{ \AA}$  in the blue wing of the  $H\alpha$  line at  $6562.8 \text{ \AA}$ . During the 3.5 h of observations (15:50-19:16 UT), we obtained 55 vector magnetograms (Figure 1), 28 Dopplergrams of the photosphere and 28  $H\alpha - 0.8 \text{ \AA}$  filtergrams of the chromosphere.

Active region NOAA 8844 consisted of two stable sunspots on January 24<sup>th</sup> and rapid growth of emerging flux in the middle of the AR were observed early on the 25<sup>th</sup>, characterized by fast moving mixed polarities with horizontal flow of  $0.3 - 0.8 \text{ km s}^{-1}$  (Bernasconi et al. 2002).

FGE  $H\alpha - 0.8 \text{ \AA}$  observations and longitudinal magnetogram ( $590 \times 590$  pixels with a  $0.18''$  pixel size) inserted in a large IVM magnetogram (Hawaii). From comparison of FGE and IVM magnetograms we have derived calibration factors for FGE. Note the dark fibrils in  $H\alpha$  blue wing (left panel) corresponding to rising motions of an arch-filament system over the emerging flux and bright points so-called Ellerman bombs (Georgoulis et al. 2002).

## 2. ELLERMAN BOMB MORPHOLOGY

$H\alpha$  observations series reveals the occurrence of numerous Ellerman bombs in the emerging flux of the AR 8844. EBS are known as fine structures with a typical 10 min life of time and characterized by

Balmer line profiles with broad wings (about  $10 \text{ \AA}$  half width in  $H\alpha$ ) and deep central absorption (Hénoux et al. 1998). This was well observed in the  $H\alpha$  spectra obtained in AR 8844 (Figure 2). The morphology and statistical properties of Ellerman bombs using FGE observations were fully investigated by Georgoulis et al. (2002a). Ellerman bombs occur and recur in preferential locations in the low chromosphere, they are associated with photospheric downflows and their loci follow the transverse mass flows on the photosphere. Their typical size is  $1.8 \times 1.1 \text{ arc sec}^2$ . A large number of Ellerman bombs are probably undetected due to limited spatial resolution and the  $H\alpha$  observations cadence (6 min). They occur in clusters which exhibit fractal properties ( $\sim 1.4$ ). Typical parameters of EBs obey power-law distribution functions with an index  $\sim -2.1$ . This suggests that EBs can contribute significantly to the heating of the low chromosphere in emerging flux regions.

## 3. LINEAR FORCE-FREE FIELD EXTRAPOLATION

Ellerman bombs are commonly explained by magnetic reconnection models, as other flaring phenomena. Recent simulations by Fang et al. (2001) show that the largest temperature rise was obtained for reconnections occurring in the middle chromosphere (600 km). The purpose of this study was to prove by a magnetic topology analysis that the EBs coincide with loci in 3D of possible magnetic reconnection.

### 3.1. Method

The magnetic field is frozen into the plasma almost everywhere in solar active regions. We assume that:

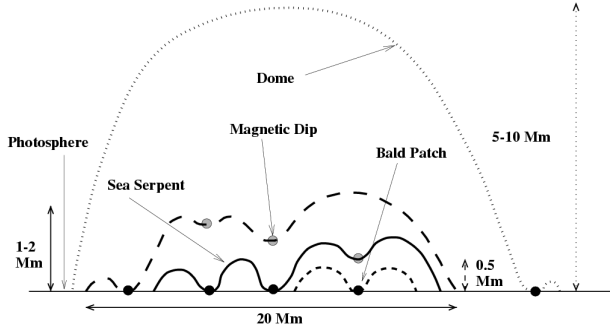


Figure 6. Sketch of the field lines overlying the emerging flux according to lfff extrapolation of the  $B_z$  magnetic field

$$\vec{\nabla} \times \vec{B} = \alpha \vec{B}$$

The current is aligned with  $\vec{B}$ , so there are no Lorentz forces.

Using a lfff extrapolation code, we obtain magnetic field lines over the AR 8844 (Démoulin et al. 1997). The field lines that fit best with TRACE coronal loops give a  $\alpha$  value for the region ( $\alpha = 0.01 \text{ Mm}^{-1}$  see Schmieder et al. 2002).

### 3.2. Association of BPs and Ellerman bombs

Separatrix surfaces are locations where current layers can be formed. Classically a separatrix is a 3D surface defined by all the field lines passing through one null point. If there are no null points another class of separatrix can be considered: then they are defined by the field lines passing through “**bald patches**” (**BPs**). BPs are regions where the vector field is tangent to the boundary (photosphere) along an inversion line. Magnetic reconnection is plausible, so local heating of the chromosphere would be expected near bald patches.

The association of BPs and Ellerman bombs was done with three different inputs. Firstly,  $B_{trans}$  was calculated from the lfff equations using **observed**  $B_{long}$ . Then, positions of bald patches (BPs) were found in the computed fields. Only a few BPs are associated with Ellerman bombs in mixed polarity regions, in the trailing spot (Figure 3) (Schmieder et al. 2002). On the other hand, BPs can be directly calculated from the **full vector field** ( $B_x$ ,  $B_y$ ,  $B_z$ ) using the  $B_{long}$  and  $B_{trans}$  observations. In that case, we found that BPs in all the regions are well associated with Ellerman bombs, including in the leading spot region, where  $B_{long} > 0$  but in which some small  $B_z < 0$  regions exist.

Finally, we have reconstructed the field lines by using lfff extrapolations from observed  $B_z$  maps, which provided not only the BP locations as the vector magnetograms do, but also the field connectivity. Thus we calculated the 3D separatrices associated to BPs, along which we also found that some EBs occurred, probably due to current intensification along the separatrices (Figure 4).

## 4. CONCLUSION

The fields in AR 8844, with its central emerging flux region, were not force-free (Georgoulis et al. 2002 b). The analysis of the magnetic topology is nevertheless possible using lfff configuration (Démoulin et al. 1997 and Aulanier et al. 1998). We calculate lfff extrapolations from observed  $B_z$  maps, they provide the “bald patch” locations and the field connectivity. Thus we calculate the 3D separatrices associated to BPs, along which EBs also occur due to current intensification along them and define the intersection lines of separatrices and the chromosphere. They are related to BPs and are aligned with a preferential direction joining the 2 main spots. Typical field lines joining BPs are so called “sea serpent”. Among the 38 EBs observed on one  $H\alpha$  map, only 5 EBs cannot be explained either by the presence of a bald patch or by the presence of separatrices. This confirms the interpretation of the observed EBs by magnetic reconnections in the low chromosphere ( $z < 1000 \text{ km}$ ). We conclude that the new flux cannot emerge along long loops, the material inside is too dense and the new field interacts with the surface convective flows. The new flux is constrained to emerge through small loops of “sea serpent” field lines with BP regions between them (Figure 6). The “sea serpent” is a succession of U loops and  $\Omega$  loops. With the rise of field lines then the “bald patches” naturally become magnetic dips which progressively vanish during the loop expansion which then become Arch Filament System.

### References:

- Aulanier, G.; Démoulin, P.; Schmieder, B.; Fang, C.; Tang, Y. H.: 1998, Solar Phys., 183, 369.
- Bernasconi P.N., Rust D.M., Eaton H.A.C., Murphy G.A.: 2000, eds. Melugin R.K. and Röser H.P., Proc. SPIE, 4014, 214
- Bernasconi P.N., Rust D.M., Murphy G.A., Eaton H.A.C.: 2001, ASP Conf Ser. 236, 399.
- Bernasconi P.N., Rust D.M., Georgoulis M.K., Labonte B.J.: 2002, Solar Phys., in press
- Chen P.F., Fang C. and Ding M.D.: 2001, Chin. J. Astron. Astrophys. Vol 1, 176
- Démoulin, P., Bagala, L. G., Mandrini, C. H., Hénoux, J. C., Rovira, M. G.: 1997, Astron. and Astrophys.: 325, 305
- Georgoulis M.K., Rust D.M., Bernasconi P.N., Schmieder B.: 2002a, ApJ, 575, 506
- Georgoulis M.K., Rust D.M., Bernasconi P.N., Schmieder B.: 2002b, AAS conf.
- Hénoux J.C., Fang C., Ding M.D.: 1998, Astron. and Astrophys. 337, 294.
- Schmieder B., Pariat E., Aulanier G., Georgoulis M.K., Rust D.M., Bernasconi P.N.: 2002, ESA, SP, in press